Dalton Transactions

ROYAL SOCIETY OF CHEMISTRY

PAPER

View Article Online
View Journal | View Issue

Cite this: *Dalton Trans.*, 2025, **54**, 10416

The effects of platinum(IV) complexes on $A\beta_{1-42}$ aggregation: a synergistic inhibition upon axial coordination†

Sara La Manna,[a] Daniele Florio,[b] James A. Platts,[c] Elisabetta Gabano,[d] Mauro Ravera[e] and Daniela Marasco *[a]

Among novel metallodrugs, Pt(IV) complexes have been receiving increasing attention as alternatives to Pt(II) analogues since they exhibit superior kinetic inertness and, hence, fewer undesirable reactions. Pt(IV) complexes have been designed as prodrugs with mechanisms of action finely tuned by properties of the axial ligands. In this context, the insertion of known bioactive molecules as axial ligands to generate multi-target drugs (MTDs) is considered a valuable drug design strategy because of the possible synergistic effects between the metal centre and the organic moiety. By employing the repurposing of drugs in different diseases, in this study, the Pt(IV) complex (*OC*-6-44)-acetatodiamminedichlorido(4,5-dihydroxy-9,10-dioxo-9,10-dihydroanthracene-2-carboxylato)platinum(IV) was investigated for its ability to modulate the self-aggregation process of the amyloid peptide $A\beta_{1-42}$. Specifically, the complex features 4,5-dihydroxy-9,10-dioxo-9,10-dihydroanthracene-2-carboxylato (rhein) as a ligand that is a natural aromatic molecule already known as a discrete inhibitor of amyloid aggregation. Herein, several biophysical and microscopic assays, such as thioflavin T (ThT) fluorescence, dynamic light scattering (DLS) and scanning electron (SEM) and confocal microscopy, indicated that the Pt(IV) complex can inhibit and disassemble $A\beta_{1-42}$ aggregation to a greater extent with respect to rhein alone. This effect is likely due to the formation of π–π interactions between the rhein moiety and the side chains of the $A\beta_{1-42}$ peptide. This experimental evidence was confirmed by molecular docking studies of monomeric and tetrameric $A\beta_{1-42}$. Overall, the data support the application of Pt(IV) complexes as innovative neurotherapeutics.

Received 21st March 2025,
Accepted 28th May 2025

DOI: 10.1039/d5dt00691k

rsc.li/dalton

[a]*Department of Pharmacy, University of Naples Federico II, 80131 Naples, Italy. E-mail: daniela.marasco@unina.it*
[b]*IRCCS SYNLAB SDN, Via G. Ferraris 144, 80146 Naples, Italy*
[c]*School of Chemistry, Cardiff University, Park Place, Cardiff CF10 3AT, UK*
[d]*Department of Sustainable Development and Ecological Transition, University of Piemonte Orientale, Piazza S. Eusebio 5, 13100 Vercelli, Italy*
[e]*Department of Sciences and Technological Innovation, University of Piemonte Orientale, Viale Michel 11, 15121 Alessandria, Italy*

† Electronic supplementary information (ESI) available: Fig. S1: stability overtime of **Pt-Ac-rhein** and **Pt-Ac-OH**; Fig. S2: time-courses of ThT fluorescence emission of $A\beta_{1-42}$, in the absence and presence of **Pt-Ac-rhein**, **Pt-Ac-OH** and **rhein** and compounds alone, and upon the addition (indicated by an arrow) of the complexes; Fig. S3: fluorescence emission spectra of Pt complexes and rhein at different times (λ_{ex} = 440 nm); Fig. S4: fluorescence emission spectra of $A\beta_{1-42}$ in the absence and presence of compound **Pt-Ac-rhein** or **rhein** at different times (λ_{ex} = 275 nm); Fig. S5: ESI-MS spectra of $A\beta_{1-42}$ in the absence and presence of **Pt-Ac-OH** and of **Pt-Ac-OH** alone; Fig. S6: ESI-MS spectra of $A\beta_{1-42}$ in the absence and presence of rhein and of rhein alone; Fig. S7: SEM analysis of $A\beta_{1-42}$ alone; Fig. S8: SEM analysis of $A\beta_{1-42}$ in the presence of **Pt-Ac-rhein**; Fig. S9: SEM analysis of $A\beta_{1-42}$ in the presence of rhein; Fig. S10: ligand interactions for the best docked complex of **Pt-Ac-rhein** with the $A\beta_{1-42}$ monomer and tetramer; and Fig. S11: best docked pose of **Pt-Ac-rhein** with the $A\beta_{1-42}$ tetramer. Table S1: table of main observed ions relative to the species formed by the $A\beta_{1-42}$ alone and mixed with **Pt-Ac-rhein**; Table S2: docking scores for **Pt-Ac-rhein**, **rhein** and **Pt-Ac-OH** with the $A\beta_{1-42}$ monomer and tetramer. See DOI: https://doi.org/10.1039/d5dt00691k

Introduction

Transition metal coordination compounds possess distinctive properties, including variable oxidation states, diverse geometries, coordination numbers, and ligands.[1–3] Over time, a large number of metal complexes have been developed and investigated for their therapeutic uses in cancer, microbial and viral infections, diabetes, and neurodegenerative diseases (NDDs).[4] Research has underscored the importance of coordination chemistry in shaping the metallodrug mechanisms of action (MOAs), which are influenced by the metal's binding preferences and ligand exchanges with functional groups from proteins and oligonucleotides.[5]

Although NDDs exhibit clinical diversity, they share key pathological characteristics, such as the cellular accumulation of intrinsically disordered proteins and disrupted metal ion homeostasis in the brain.[6] While significant advances have been made in understanding these diseases and developing treatments, to date no definitive cures have been achieved.[7] The abnormal formation of oligomers and fibrils through the self- or hetero-assembly of amyloidogenic systems—such as

amyloid-β, α-synuclein, huntingtin, tau, and islet amyloid polypeptides—is directly implicated in NDDs like Alzheimer's, Parkinson's, and Huntington's diseases, as well as frontotemporal dementia and type II diabetes.[8]

Accurately designed metal complexes can stabilize alternative, non-toxic conformations of amyloid proteins by inhibiting fibril formation, or promote disaggregation of existing aggregates.[9,10] Among others, Pt-based compounds have been explored for this purpose: several complexes inhibited amyloid aggregation and modulated their toxicity[11–14] through a predominantly coordinative MOA, targeting as metal-binding sites the histidine residues (in $A\beta_{1-42/1-40}$: His^6, His^{13}, and His^{14}).[15] Studies demonstrated that the charge, the steric hindrance and aromatic features around Pt(II) exert pivotal roles in tuning the MOAs of these complexes. For example, Pt(II) complexes, containing the 1,10-phenanthroline ligands, modulated $A\beta_{1-42}$ peptide aggregation and reduced neurotoxicity in mouse hippocampal tissue by coordinating His residues.[16] In recent studies, Pt(II) complexes with β-hydroxy dithiocinnamic esters as ligands have been shown to inhibit the aggregation of different amyloid models such as $NPM1_{264-277}$, the heptapeptide GNNQQNY from the Yeast Prion Protein Sup35p ($Sup35p_{7-13}$) and $A\beta_{21-40}$ fragments.[17–20] The limited solubility in aqueous solutions of these initial complexes hindered their development into viable therapeutic drugs; consequently, other studies have been focused on the use of water-soluble Pt(II) complexes. The incorporation of the tridentate ligand terpyridine in the square-planar structure of Pt(II) complexes to obtain (*SP*-4-2)-chlorido(2,2′:6′,2″-terpyridine)platinum(II) chloride (Pt-terpy) aided the inhibition of $A\beta_{21-40}$ aggregation.[21] Consistently, the role of charge has been further investigated with positive and neutral complexes that demonstrated their ability as efficient inhibitors of $A\beta_{21-40}$ aggregation, which reduced peptide cytotoxicity in SH-SY5Y neuroblastoma cells.[22] In this *scenario*, two glycoconjugate Pt(II) bipyramidal complexes suppressed amyloid aggregation of the polypeptide fragments $A\beta_{21-40}$ and $A\beta_{25-35}$.[23]

In the search for different interaction modes between amyloid proteins and metal complexes, the peculiar features of Pt(IV) complexes can be explored. These octahedral compounds are actively studied as anticancer drugs because they are more inert than traditional Pt(II) compounds and require activation by reduction *in vivo* in the hypoxic tumor tissue, making them potentially more selective and less toxic, and producing fewer adverse effects than Pt(II) complexes,[24–26] also making them applicable in the amyloid context.[27] Moreover, the octahedral coordination geometry makes the introduction of one or two bioactive ligands possible in the axial positions, producing potentially multi-functional agents combining the MOA of the platinum moiety with that of the bioactive ligands in an additive or, better, synergistic way.[28] In this context, to generate a suitable complex, the well-known cisplatin was combined with a molecule of rhein (4,5-dihydroxy-9,10-dioxo-9,10-dihydroanthracene-2-carboxylic acid or cassic acid) and an acetate group to complete the coordination, thus providing the compound (*OC*-6-44)-acetatodiamminedichlorido(4,5-dihydroxy-9,10-dioxo-9,10-dihydroanthracene-2-carboxylato)platinum(IV), nicknamed **Pt-Ac-rhein** (Fig. 1).[29] This complex proved to be similar to or more potent than the parent cisplatin and rhein compounds on two human glioblastoma cell lines (U87-MG and T98G). Importantly, physicochemical and computational studies indicated its superior ability to cross the blood–brain barrier than rhein itself.[29] The rhein molecule alone demonstrates several pharmacological effects, such as anti-inflammatory, anti-fibrosis, anti-oxidant and anticancer abilities, manifested by modulating cell proliferation, apoptosis, migration, and invasion.[30,31] It has been demonstrated that rhein can partially dissociate or antagonize the oligomerization of class A scavenger receptors (SCARA). SCARA is a class of cell surface receptors involved in cell adhesion and uptake of ligands and are expressed on microglia and astrocytes. The first member of the SCARA family, SCARA-1, exhibited high interaction levels around the Aβ plates in microglial cells. Docking and molecular dynamic simulations indicated that both hydrophobic and H-bonds are responsible for these interactions.[32,33] Importantly, rhein demonstrated a discrete ability to inhibit $A\beta_{1-42}$ amyloid aggregation, where its carboxylic group is able to interact with Lys^{16} and Lys^{28} residues and these direct interactions targeted the monomer, dimer, and trimer, further suppressing oligomerization.[34]

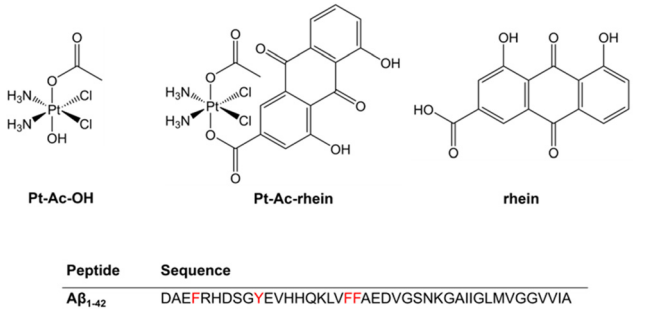

Fig. 1 Structure of the compounds and sequence of the $A\beta_{1-42}$ investigated in this study. The aromatic amino acids of the amyloid polypeptide are highlighted in red.

In light of the above considerations, the ability of **Pt-Ac-rhein** to interfere with the aggregation of $A\beta_{1-42}$ was investigated *via* a range of spectroscopic and microscopic techniques, as well as by molecular dynamics (MD) methods. The complex **Pt-Ac-OH**, as the precursor of **Pt-Ac-rhein**, and rhein were included in the study in order to distinguish between the effects of the separate moieties.

Results and discussion

Modulation of $A\beta_{1-42}$ aggregation

Prior to performing amyloid-related assays, the stability of **Pt-Ac-rhein** and **Pt-Ac-OH** was evaluated by registering UV-vis absorption spectra at different times and at three concentrations (Fig. S1†). **Pt-Ac-OH** was stable at all tested concentrations, up to 24 h (Fig. S1B†). Regarding **Pt-Ac-rhein**, the almost complete superimposition of the spectra at 25 and

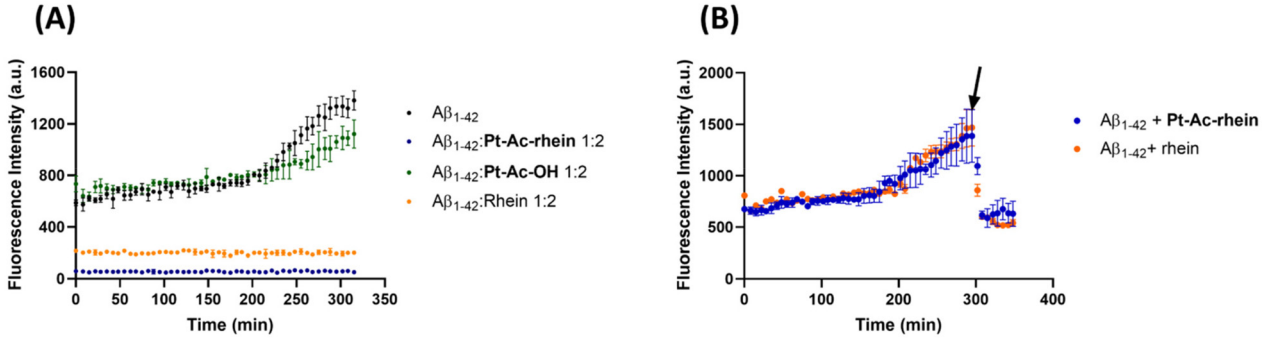

Fig. 2 Overlay of time-courses of ThT fluorescence emission intensity of (A) $A\beta_{1-42}$, in the absence and presence of **Pt-Ac-rhein**, **Pt-Ac-OH** and **rhein**, and (B) upon the addition (indicated by an arrow) of the complexes at a 1 : 1 molar ratio to pre-formed amyloid aggregates. The results are representative of three independent measurements.

50 μM indicated great stability of the complex, while at 100 μM, a certain variability of absorbance suggested potential aggregation over time (Fig. S1A†).

To analyze the effects of these compounds on the self-recognition process of $A\beta_{1-42}$, thioflavin T (ThT) binding assay was employed,[35–37] and experiments were carried out by adding both compounds at the beginning of aggregation and once oligomers had become pre-formed (Fig. 2). The time course profiles of the ThT fluorescence of $A\beta_{1-42}$ alone and in the presence of compounds are reported in Fig. 2A. The $A\beta_{1-42}$ peptide alone exhibited a typical sigmoidal profile presenting a $t_{\frac{1}{2}}$ value of ~250 min. The effects of the presence of **Pt-Ac-rhein** were analyzed at two different peptide : complex molar ratios (1 : 1 Fig. S2A† and 1 : 2 Fig. 2A) and, in both cases, the complex showed a clear inhibitory effect reducing the maximum fluorescence value at 150 a.u. with an average inhibition of ~90%. A similar, but less marked, effect was observed in the presence of **rhein** with a fluorescence value of 255 a.u. and 20% inhibition (Fig. 2A). **Pt-Ac-OH** showed a negligible effect, presenting ThT profiles almost superimposable on those of the peptide alone at both tested ratios (Fig. 2A and S2A†). None of the compounds exhibited interference with ThT (Fig. S2A†). Control emission spectra of compounds alone, λ_{ex} = 440 nm, are reported in Fig. S3.†

Having assessed the suppressive abilities of compounds toward amyloid aggregation starting from monomers, their effects on pre-formed oligomers were evaluated by monitoring the ThT signals after the addition of compounds to $A\beta_{1-42}$ aggregates in a 1 : 1 peptide : compound molar ratio (Fig. 2B). Upon the addition of the compounds, both **Pt-Ac-rhein** and **rhein** caused a decrease in ThT fluorescence intensity, with an inhibitory effect of ~60%. Conversely, the addition of **Pt-Ac-OH** had no effect on the pre-formed aggregates (Fig. S2A†).

The lack of effect of **Pt-Ac-OH** led us to speculate on a potential aromatic effect among the anthracene portion of rhein and aromatic residues of the polypeptide sequence as Phe at positions 4, 19 and 20, and Tyr at position 10. To gain insights into this aspect, the fluorescence emission of $A\beta_{1-42}$, upon excitation at 275 nm, in the presence and absence of the investigated compounds, was recorded. As displayed in Fig. S4,† the $A\beta_{1-42}$ alone shows a progressive decrease in its fluorescence intensity at 303 nm over time, as previously observed.[41] The presence of rhein and in particular of **Pt-Ac-rhein** already causes a significant reduction of this signal at t = 0 h, suggesting involvement of aromatic residues in the interaction with the compounds and thus important contributions of π–π bonds in the inhibition of aggregation observed.

ESI-MS analysis of adducts between complexes and $A\beta_{1-42}$

To evaluate direct interaction between $A\beta_{1-42}$ and the investigated compounds, native electrospray ionization mass spectrometry (ESI-MS) was used. $A\beta_{1-42}$ was incubated with the compounds (at 1 : 1 molar ratio) (Fig. 3); $A\beta_{1-42}$ and Pt(IV) compounds alone were analyzed as references. As can be observed, in the presence of **Pt-Ac-rhein**, two additional peaks, with respect to $A\beta_{1-42}$ alone, were found at m/z 1719.12 and 1290.76 a.m.u. (Table S1†). These peaks were attributed to the formation of a non-covalent adduct between $A\beta_{1-42}$ and one **Pt-Ac-rhein** molecule.

Conversely, in the presence of **Pt-Ac-OH** (Fig. S5†), no adduct formation was observed, nor was there any formation in the presence of rhein (Fig. S6†). Because of the observed inefficacy of the **Pt-Ac-OH** complex to modulate $A\beta_{1-42}$ aggregation, it was not included in subsequent experiments. The absence of any adduct in the case of **Pt-Ac-OH** is likely due to the lack of potential of aromatic interactions between the complex and the polypeptide.

Effects of Pt(IV) complexes on amyloid $A\beta_{1-42}$ aggregation: DLS assay

Dynamic light scattering (DLS) was employed to evaluate the effects of compounds on the size of $A\beta_{1-42}$ aggregates (Fig. 4). Correct autocorrelation of the native $A\beta_{1-42}$ was achieved after 24 h with a diameter of ~155 nm (Fig. 4A) as already reported.[38,42,43] Conversely, the presence of **Pt-Ac-rhein** (1 : 1 molar ratio) anticipated autocorrelation at t = 0 h, by stabilizing greater oligomers centered at ~1130 nm (Fig. 4B). Smaller diameters, compatible with the peptide alone, are also

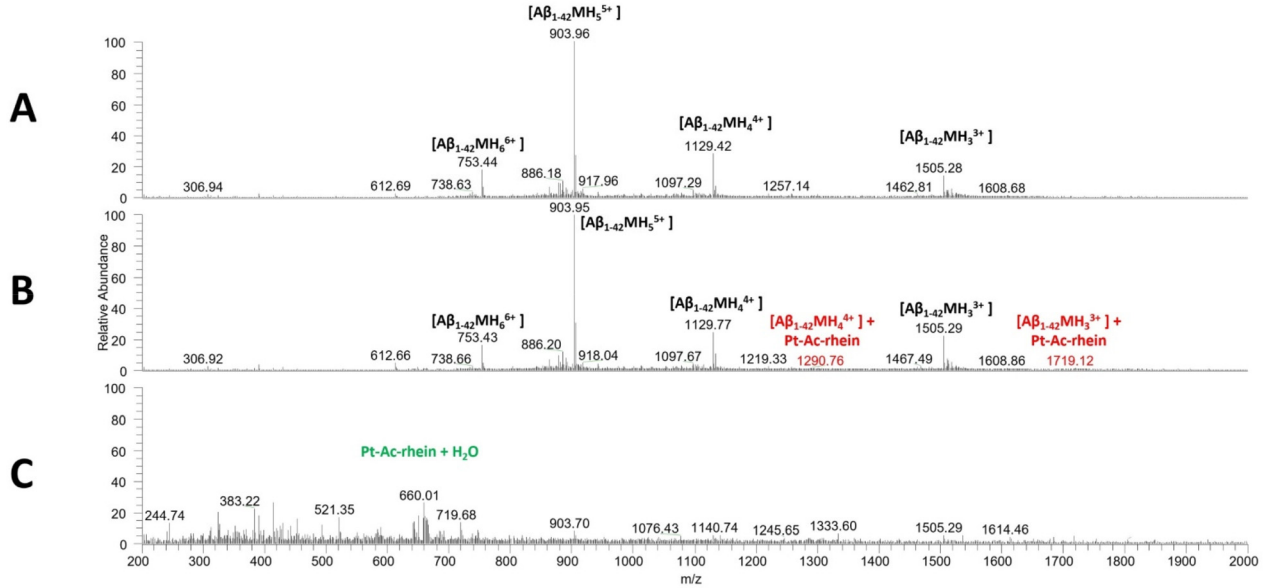

Fig. 3 ESI-MS spectra of $A\beta_{1-42}$ (A) in the absence and (B) presence of **Pt-Ac-rhein**, and (C) the spectrum of the latter compound alone.

observed. Potential differences in the surface charges of monomers and/or small oligomers can lead, in the presence of **Pt-Ac-rhein**, to the formation of oligomers that are larger than those formed by $A\beta_{1-42}$ alone. The small variation in the sizes of oligomers formed over time falls within the error of the measurement. DLS data suggest that the adduct formed by **Pt-Ac-rhein** and $A\beta_{1-42}$ stabilizes oligomeric states, which are unable to further oligomerize.[38,39] Samples derived from the incubation of $A\beta_{1-42}$: rhein at 1 : 1 ratio, rhein and **Pt-Ac-rhein** alone did not correlate (data not shown). The inability to correlate the $A\beta_{1-42}$: rhein sample does not imply lack of interaction of rhein with $A\beta_{1-42}$, but instead indicates that this interaction was insufficient to stabilize definitive sizes of amyloid aggregates.

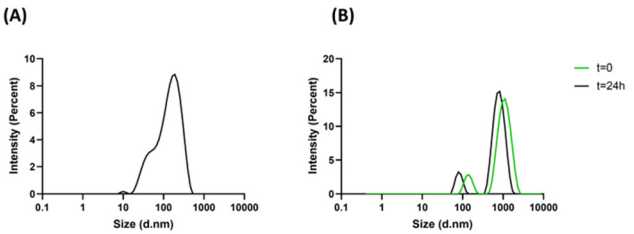

Fig. 4 Overlay of size distribution by DLS measurements of the native $A\beta_{1-42}$ peptide at t = 24 h (A) and with the complex **Pt-Ac-rhein** (B) at an Aβ : complex mole ratio of 1 : 1, at t = 0 (green line) and t = 24 h (black line).

Effects of metal complexes on the morphologies of amyloid fibers

Potential modifications of the morphology of $A\beta_{1-42}$ aggregates induced by **Pt-Ac-rhein** and **rhein** alone were studied by using the technique of scanning electron microscopy (SEM). Samples, prepared by mixing at a 1 : 1 molar ratio, were analyzed across four independent experiments, with the images from one representative experiment being shown in Fig. 5. Additional data from the other independent experiments are presented in Fig. S7–S9.† As expected, after 6 h of stirring, the $A\beta_{1-42}$ peptide alone provides well-defined fibers with an average length of ~1040 μm and a diameter of ~13 μm (Fig. 5 upper panel, Table 1). In the presence of **Pt-Ac-rhein**, a significant reduction in fiber diameter (~8 μm) and a change in their morphology were evident; indeed, the fiber appeared folded back several times, making measurement of its length impossible (Fig. 5B–B″). In the presence of rhein, a fiber with a diameter comparable to that of the peptide alone was observable, but with a length approximately 7 times shorter. The amyloid character of the observed aggregates in SEM was corroborated by confocal microscopy analysis (Fig. 5, lower panel). In the case of $A\beta_{1-42}$ alone and with rhein, fibers, although different in size, demonstrated incorporation of ThT, confirming their amyloid character (Fig. 5, lower panel, D–G). Conversely, for $A\beta_{1-42}$ with **Pt-Ac-rhein**, the low fluorescence intensity observed (Fig. 5, lower panel, E–G) confirmed the amorphous nature of the observed aggregates.

Modelling studies of the interaction of Pt-Ac-rhein with $A\beta_{1-42}$

Pt-Ac-rhein was docked into monomeric and tetrameric $A\beta_{1-42}$, along with rhein and **Pt-Ac-OH**, as controls. To reflect the intrinsically disordered nature of $A\beta_{1-42}$, docking was carried out using 10 different conformations of the monomer.[40] As reported in Table S2,† **Pt-Ac-rhein** forms stable adducts in 1 : 1 complexes, each of which are significantly more stable than equivalent forms involving either rhein or **Pt-Ac-OH**. It is apparent that the conjugation of rhein with the Pt(IV) center gives rise to markedly greater interaction with $A\beta_{1-42}$ than rhein alone. **Pt-Ac-rhein** is more strongly bound to the $A\beta_{1-42}$

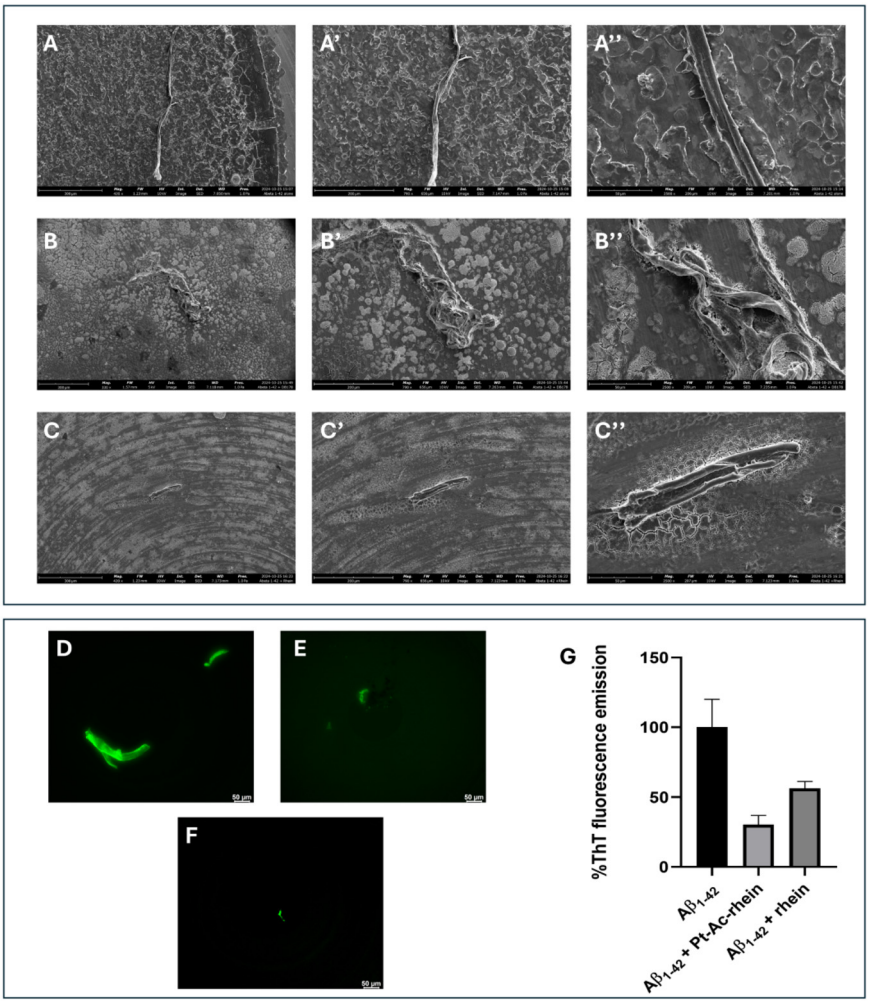

Fig. 5 Upper panel: scanning electron microscopy images of $A\beta_{1-42}$ alone (A) and in the presence of **Pt-Ac-rhein** (B) and **rhein** (C) at a magnification of 330× (300 μm scale bar, A, B, and C), 790× (200 μm scale bar, A′, B′, and C′) and 2500× (50 μm scale bar, A″, B″, and C″). Lower panel: confocal microscopy images (λ_{ex} = 440 nm and λ_{em} = 480 nm) of $A\beta_{1-42}$ alone (D) and in the presence of **Pt-Ac-rhein** (E) and **rhein** (F) at a magnification of 10×. (G) Histogram showing the percentage of ThT fluorescence intensity from confocal analysis. The SEM images are representative of four independent experiments (the images from other experiments are shown in Fig. S7–S9†).

Table 1 SEM analyses: average diameter and length of fibers obtained for $A\beta_{1-42}$ in the presence and absence of **Pt-Ac-rhein** and **rhein**. Values represent the mean from four independent experiments: one representative experiment is shown in Fig. 5 and the others are presented in Fig. S7–S9†

	Average diameter (μm)	Average length (μm)
$A\beta_{1-42}$	13 ± 2	1040 ± 3.0
$A\beta_{1-42}$:**Pt-Ac-rhein**	7.4 ± 2	Could not be evaluated
$A\beta_{1-42}$:**rhein**	18.6 ± 0.5	146 ± 0.9

monomer than rhein alone with a ChemPLP score of ~10 on average.

In the 1 : 1 **Pt-Ac-rhein** complex, intermolecular interactions occur largely within the N-terminal region of $A\beta_{1-42}$. This is particularly evident in the complex indicated with monomer 8 in Table S2† (Fig. 6), in which strong polar interactions between coordinated $-NH_3$ groups and sidechains of Asp^1 and Glu^3 as well as backbone carbonyl of Ala^2 are evident. In addition, stacking interactions between the rhein moiety and Phe^4 and His^6 are observed (Fig. S10†). Thus docking provides evidence that the combination of a polar Pt(IV) complex with an extended aromatic ligand forms an excellent combination for binding to monomeric $A\beta_{1-42}$.

Docking was also performed on 5 representative clusters as tetramers of $A\beta_{1-42}$ reported by Nguyen *et al.*[41] (Table S2†). Again, it is apparent that **Pt-Ac-rhein** binds significantly more strongly than either of rhein or **Pt-Ac-OH** alone. As in the monomer case, the most stable 1 : 4 complex located by docking is stabilized by polar interactions between coordinated $-NH_3$ groups and acidic residues in $A\beta_{1-42}$, particularly Glu^3 and Glu^{22} of chain A. Hydrophobic interactions also form between the rhein moiety and Phe^4, Phe^{19} and Phe^{20} of chain A (Fig. 7 and S10†): **Pt-Ac-rhein** slots between helical and sheet structures

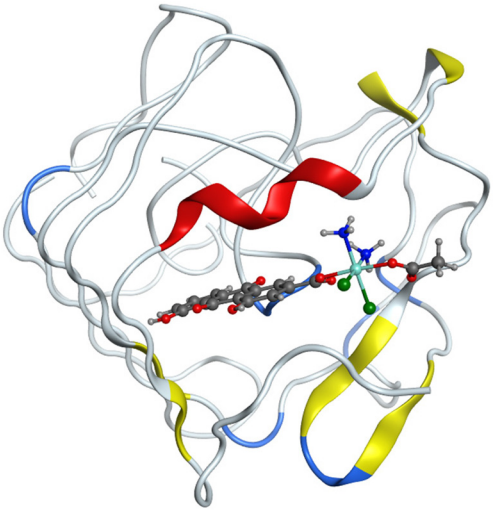

Fig. 6 Best docked pose of **Pt-Ac-rhein** with the $A\beta_{1-42}$ monomer. **Pt-Ac-rhein** is shown as a ball-and-stick model, and residues Asp^1, Ala^2, Glu^3, Phe^4 and His^6 are shown as stick models. The peptide is colored yellow for β-strands, blue for turns/bends, and white for random coils.

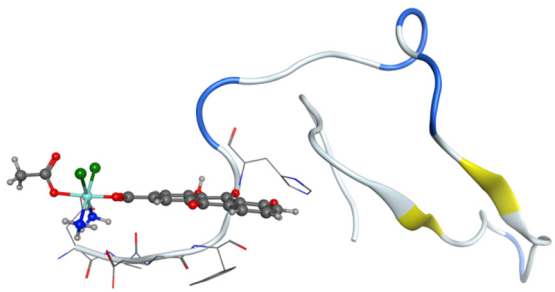

Fig. 7 Best docked pose of **Pt-Ac-rhein** with the $A\beta_{1-42}$ tetramer. **Pt-Ac-rhein** is shown as a ball-and-stick model. The peptide is colored red for the helix, yellow for β-strands, blue for turns/bends, and white for random coils.

formed by chain A on the surface of the tetramer. A surface representation of the receptor colored on the basis of lipophilicity (Fig. S11†) shows how this binding pose includes hydrophilic pockets formed by Glu residues, as noted above, while the rhein group slots into a hydrophobic pocket formed by Phe residues. As in the monomer case, **Pt-Ac-rhein** is predicted to bind more strongly than rhein alone with a ChemPLP score of ~10 on average, with **Pt-Ac-OH** alone being even less strongly bound. This is in agreement with the high lipophilicity of **Pt-Ac-rhein**, measured in an *n*-octanol/water system and expressed as distribution coefficient *D*, to compare neutral **Pt-Ac-rhein** ($\log D$ = 1.85) with ionizable rhein ($\log D$ = −0.27).[29]

Experimental

Synthesis of peptides

The $A\beta_{1-42}$ polypeptide was purchased from NovoPro Bioscience Inc. (Shanghai, China). The peptide was treated with 1,1,1,3,3,3-hexafluoro-2-propanol (HFIP) to guarantee a monomeric state, lyophilized and stored at −20 °C until use.[42]

Synthesis of metal compounds

4,5-Dihydroxy-9,10-dioxo-9,10-dihydroanthracene-2-carboxylic acid or rhein (Tokyo Chemical Industry) and all the other chemicals (Alfa Aesar; Thermo Fisher Scientific or Sigma Aldrich; Merck) were used without further purification. Cisplatin was prepared according to Dhara's method.[43] Complex (*OC*-6-44)-acetatodiamminedichloridohydroxidoplatinum(IV), **Pt-Ac-OH**, was prepared by treating cisplatin (100 mg) with 50% w/w oxygen peroxide (1 mL) in acetic acid (40 mL) as previously described.[44,45] Complex (*OC*-6-44)-acetatodiamminedichlorido(4,5-dihydroxy-9,10-dioxo-9,10-dihydroanthracene-2-carboxylato)platinum(IV), **Pt-Ac-rhein**, was prepared as reported in the literature.[29] Briefly, **Pt-Ac-OH** (0.100 g) was reacted with rhein (0.091 g) in the presence of 1-[bis(dimethylamino) methylene]-1*H*-1,2,3-triazolo[4,5-*b*]pyridinium 3-oxide hexafluorophosphate (HATU, 0.145 g) and *N*,*N*-diisopropylethylamine (50 μL) in anhydrous DMF (3 mL) overnight. Upon centrifugation of the mixture, the volume of the supernatant was reduced using a rotary evaporator. The oily residue was triturated with a dichloromethane–diethyl ether mixture to give a yellow powder, which was washed with diethyl ether, 1% formic acid and cold water, and finally dried under nitrogen flow (58% yield).

UV-vis absorption spectroscopy

The solution stability of **Pt-Ac-rhein** and **Pt-Ac-OH** was evaluated by recording their UV-vis absorption spectra in 10 mM phosphate buffer at pH 7.4 over 24 hours. To record the spectra, the compounds were dissolved in DMSO (stock solutions 50 mM) and then added to the selected buffers to reach a final concentration of 25, 50 or 100 μM. The DMSO final concentration was 0.2% v/v. UV-vis absorption spectra were recorded on BioDrop Duo UV–visible spectrophotometers (Cambridge, United Kingdom), at room temperature, using 1 cm path length cuvettes and the following parameters: 350–600 nm range, 200 nm min^{-1} scanning speed, and 2.0 nm bandwidth.

Fluorescence spectroscopy

The ThT emission assay was carried out on an EnVision 2105 fluorescence reader (PerkinElmer) using black plates (96 well) while stirring. Measurements were recorded every 8 min (λ_{ex}: 440 nm and λ_{em}: 485 nm). Assays were performed at 25 °C employing a peptide concentration of 50 μM (buffer composition: 50 mM NaCl and 20 mM phosphate buffer, pH 7.4), using a ThT final concentration of 5 μM, at different molar ratios with metal complexes (stock solutions of 50 mM in DMSO, final DMSO concentration of 0.2% v/v). For disaggregation experiments, the fibrillation of $A\beta_{1-42}$ was carried out by mixing the peptide at the desired concentration with ThT, in 50 mM NaCl and 20 mM phosphate buffer, at pH 7.4, and the solution was placed in the black plates, kept under agitation and moni-

tored; metal complexes were added when maximum fibrillation was reached.

Intrinsic fluorescence was carried out using 50 μM $A\beta_{1-42}$ mixed with the compounds at a 1 : 1 molar ratio (peptide : compound), in a quartz cuvette with an optical path length of 10 mm, on a Jasco FP 8300 spectrofluorometer (λ_{ex} = 275 nm).

ESI-MS analysis

The solution of $A\beta_{1-42}$ at a concentration of 50 μM in 15 mM ammonium acetate (AMAC) buffer at pH = 7.0 was incubated with **Pt-Ac-rhein** and **Pt-Ac-OH** in a peptide to metal compound molar ratio of 1 : 1. The solutions were diluted 10 times with 15 mM AMAC and then analyzed using an LTQ XL Ion Trap mass spectrometer equipped with an electrospray ionization (ESI) source, operating at a needle voltage of 3.5 kV and temperature of 320 °C, combined with a complete Ultimate 3000 HPLC system, including a pump MS, autosampler, and photodiode array (all from Thermo Fisher Scientific). Spectra of the complexes alone were recorded as controls.

DLS assays

DLS measurements were performed using a Zetasizer Nano S DLS device from Malvern Instruments (Malvern, Worcestershire, UK) equipped with a 633 nm laser, at a backscatter angle of 173°, controlled with a Peltier thermostat system while using a plastic micro cuvette. $A\beta_{1-42}$ at a concentration of 50 μM in 50 mM NaCl and 20 mM phosphate buffer (pH 7.4) was maintained under conditions of stirring at 25 °C either alone or at a 1 : 1 peptide-to-metal complex molar ratio on a Multi Reax Vortexer 115 V (Heidolph Instruments GmbH & Co., Schwabach, Germany). Size distribution values were determined by intensity measurements in automatic mode at regular time-intervals over a period of 10 min for each measurement. Thirteen acquisitions were recorded, each of 10 seconds in duration.

Scanning electron microscopy

$A\beta_{1-42}$ alone (50 μM) and in the presence of compounds **Pt-Ac-rhein** and rhein (1 : 1 peptide : complex molar ratio) in 10 mM phosphate buffer, pH 7.4, were morphologically analyzed after 6 h of aggregation using field-emission SEM (Phenom_XL, Alfatest, Milan, Italy). The aggregation was achieved by maintaining the solutions under stirring conditions at 25 °C on a Multi Reax Vortexer 115 V (Heidolph Instruments GmbH & Co., Schwabach, Germany) for 6 h. After this time, ~50 μL of solution was drop-cast on an aluminum stub and this was dried under vacuum to prepare each sample. For 75 s, a thin layer of gold was sputtered at a current of 25 mA. Following the introduction of the sputter-coated samples into the specimen chamber, micrographs were obtained using a secondary electron detector (SED) at an accelerating voltage of 10 kV. The **Pt-Ac-rhein** (50 μM) and rhein (50 μM) compounds were analyzed as controls.

Confocal microscopy

Confocal microscopy analysis was performed using a Leica X Mica Microhub. $A\beta_{1-42}$ (50 μM), either alone or mixed with **Pt-Ac-rhein** or rhein at 1 : 1 molar ratio, was first incubated with 50 μM ThT in 50 mM NaCl and 20 mM phosphate buffer (pH 7.4) at room temperature for 6 h, under conditions of stirring. After incubation, the fluorescence of the formed fibers was analyzed using the excitation wavelength of ThT at 440 nm, with the detection occurring at 483 nm. Fluorescence images were acquired using a 10× objective with the pinhole set to its maximum opening. The percentages of the ThT fluorescence intensity signals were analyzed using the image processing program ImageJ.

Computational methods

Geometries of **Pt-Ac-rhein**, rhein and **Pt-Ac-OH** were fully optimized at the B3LYP-G3BJ level with a def2-SVP basis set without any symmetry constraint, and confirmed as minima by harmonic frequency calculation. Single point calculations at the optimal geometry were then performed at the B3LYP/def2-TZVP level to obtain atomic charges using the Merz–Kollman scheme. Each structure, as determined, was then docked into receptors consisting of different conformations of monomeric or tetrameric $A\beta_{1-42}$ taken from the literature. Docking employed the PLANTS program,[46] with the entire structure of the monomer or tetramer taken as the receptor.

Conclusion

In recent years transition metal complexes have garnered significant attention for their potential applications in the diagnosis, imaging, and treatment of NDDs.[47] Very few studies have reported on metal complexes bearing Pt(IV) coordination as modulators of amyloid aggregation. In this study, to exploit potential synergistic effects, a molecule of natural origin that exhibited discrete inhibitory effects on $A\beta_{1-42}$ was included as an axial ligand into an octahedral Pt(IV) species to obtain the complex named **Pt-Ac-rhein**. This complex was investigated to determine its effects toward amyloid aggregation in comparison with the parent metal complex lacking the rhein ligand, **Pt-Ac-OH**, and the rhein molecule alone (Fig. 1). ThT and aromatic assays indicated that **Pt-Ac-rhein** was able to drastically suppress aggregation and disassemble pre-formed high-level oligomers. DLS studies suggested a MOA involving the stabilization of large oligomers induced by the presence of **Pt-Ac-rhein** and these were unable to further form amyloid fibrils, as indicated by SEM and confocal images. Mass spectrometry showed that **Pt-Ac-rhein** directly interacts with $A\beta_{1-42}$ for the formation of a non-covalent adduct between the complex and the amyloid polypeptide without exchange of ligands around Pt(IV), as expected. The presence of rhein in the coordination sphere of Pt(IV) allows for π–π interactions with aromatic residues of the amyloid sequence, as shown by docking simulations with both monomeric and tetrameric forms of $A\beta_{1-42}$. These interactions presumably stabilize the formation of

adducts with $A\beta_{1-42}$ as the monomer as well as small oligomers, hampering further aggregation. The superior inhibitory effect observed for **Pt-Ac-rhein** with respect to rhein alone could be ascribed to the precise geometrical position of rhein in the context of the metal complex as an axial ligand in the octahedral geometry around Pt(IV), which can enhance π–π interactions and/or allow the stabilization of soluble oligomers of $A\beta_{1-42}$.

Unfortunately, the intrinsic cytotoxicity of **Pt-Ac-rhein** observed in human glioblastoma cell lines, with IC_{50} values in the low micromolar range, hampered any cytotoxicity assay to evaluate potential rescue of cell viability due to the suppression of amyloid aggregation.[29] However, to the best of our knowledge, this is the first investigation of a Pt(IV) complex incorporating rhein as the axial ligand specifically in relation to its anti-amyloidogenic properties. In conclusion, this study provides critical information on the inhibition of amyloid fibrillation by Pt(IV) metal complexes with unprecedented impact on the biomedical value of clinical metal-based MTDs against amyloid diseases.

Author contributions

Funding acquisition, conceptualization, and original draft: D. M.; supervision, review and editing: D.M. and M.R.; investigation and formal analysis: S.L.M., D.F., E.G., and J.A.P.

Data availability

The data supporting this article have been included as part of the ESI.†

Conflicts of interest

There are no conflicts to declare.

Acknowledgements

This work was supported by the Associazione Italiana per la Ricerca sul Cancro (AIRC) grant IG 2022, Rif. 27378 (D. M.) and by #NEXTGENERATIONEU (NGEU), the Ministry of University and Research (MUR), the National Recovery and Resilience Plan (NRRP), project MNESYS (PE0000006) – A multiscale integrated approach to the study of the nervous system in health and disease (DN. 1553 11.10.2022). D. F. acknowledges the Italian Ministry of Health – Ricerca Corrente Project.

References

1 G. Son, B. I. Lee, Y. J. Chung and C. B. Park, Light-triggered dissociation of self-assembled beta-amyloid aggregates into small, nontoxic fragments by ruthenium(II) complex, *Acta Biomater.*, 2018, **67**, 147–155.
2 J. M. Suh, G. Kim, J. Kang and M. H. Lim, Strategies Employing Transition Metal Complexes To Modulate Amyloid-beta Aggregation, *Inorg. Chem.*, 2019, **58**, 8–17.
3 P. K. Wan, K. C. Tong, C. N. Lok, C. Zhang, X. Y. Chang, K. H. Sze, A. S. T. Wong and C. M. Che, Platinum(II) N-heterocyclic carbene complexes arrest metastatic tumor growth, *Proc. Natl. Acad. Sci. U. S. A.*, 2021, **118**, e2025806118.
4 I. Yousuf, M. Bashir, F. Arjmand and S. Tabassum, Advancement of metal compounds as therapeutic and diagnostic metallodrugs: Current frontiers and future perspectives, *Coord. Chem. Rev.*, 2021, **445**, 214104.
5 M. A. Telpoukhovskaia and C. Orvig, Werner coordination chemistry and neurodegeneration, *Chem. Soc. Rev.*, 2013, **42**, 1836–1846.
6 C. Ma, F. Hong and S. Yang, Amyloidosis in Alzheimer's Disease: Pathogeny, Etiology, and Related Therapeutic Directions, *Molecules*, 2022, **27**, 1210.
7 C. Soto and S. Pritzkow, Protein misfolding, aggregation, and conformational strains in neurodegenerative diseases, *Nat. Neurosci.*, 2018, **21**, 1332–1340.
8 T. D. Samdin, A. G. Kreutzer and J. S. Nowick, Exploring amyloid oligomers with peptide model systems, *Curr. Opin. Chem. Biol.*, 2021, **64**, 106–115.
9 F. Daniele, D. Marasco and S. La Manna, Approaches for developing peptide-and metal complexes-or chelators-based leads for anti-amyloid drugs, *Inorg. Chim. Acta*, 2024, 122474.
10 D. Florio, I. Iacobucci, G. Ferraro, A. M. Mansour, G. Morelli, M. Monti, A. Merlino and D. Marasco, Role of the metal center in the modulation of the aggregation process of amyloid model systems by square planar complexes bearing 2-(2′-pyridyl) benzimidazole ligands, *Pharmaceuticals*, 2019, **12**, 154.
11 M. P. Decatris, S. Sundar and K. J. O'Byrne, Platinum-based chemotherapy in metastatic breast cancer: current status, *Cancer Treat. Rev.*, 2004, **30**, 53–81.
12 H. Liu, Y. Qu and X. Wang, Amyloid beta-targeted metal complexes for potential applications in Alzheimer's disease, *Future Med. Chem.*, 2018, **10**, 679–701.
13 E. Babu, J. Bhuvaneswari, K. Rajakumar, V. Sathish and P. Thanasekaran, Non-conventional photoactive transition metal complexes that mediated sensing and inhibition of amyloidogenic aggregates, *Coord. Chem. Rev.*, 2021, **428**, 213612.
14 J. H. Viles, Metal ions and amyloid fiber formation in neurodegenerative diseases. Copper, zinc and iron in Alzheimer's, Parkinson's and prion diseases, *Coord. Chem. Rev.*, 2012, **256**, 2271–2284.
15 V. A. Streltsov, V. C. Epa, S. A. James, Q. I. Churches, J. M. Caine, V. B. Kenche and K. J. Barnham, Structural insights into the interaction of platinum-based inhibitors with the Alzheimer's disease amyloid-β peptide, *Chem. Commun.*, 2013, **49**, 11364–11366.

16 K. J. Barnham, V. B. Kenche, G. D. Ciccotosto, D. P. Smith, D. J. Tew, X. Liu, K. Perez, G. A. Cranston, T. J. Johanssen and I. Volitakis, Platinum-based inhibitors of amyloid-β as therapeutic agents for Alzheimer's disease, *Proc. Natl. Acad. Sci. U. S. A.*, 2008, **105**, 6813–6818.

17 S. La Manna, V. Roviello, P. L. Scognamiglio, C. Diaferia, C. Giannini, T. Sibillano, G. Morelli, E. Novellino and D. Marasco, Amyloid fibers deriving from the aromatic core of C-terminal domain of nucleophosmin 1, *Int. J. Biol. Macromol.*, 2019, **122**, 517–525.

18 M. Balbirnie, R. Grothe and D. S. Eisenberg, An amyloid-forming peptide from the yeast prion Sup35 reveals a dehydrated β-sheet structure for amyloid, *Proc. Natl. Acad. Sci. U. S. A.*, 2001, **98**, 2375–2380.

19 L. L. Iversen, R. J. Mortishire-Smith, S. J. Pollack and M. S. Shearman, The toxicity in vitro of beta-amyloid protein, *Biochem. J.*, 1995, **311**, 1.

20 D. Florio, A. M. Malfitano, S. Di Somma, C. Mugge, W. Weigand, G. Ferraro, I. Iacobucci, M. Monti, G. Morelli, A. Merlino and D. Marasco, Platinum(II) O,S Complexes Inhibit the Aggregation of Amyloid Model Systems, *Int. J. Mol. Sci.*, 2019, **20**, 829.

21 S. Manna, D. Florio, I. Iacobucci, F. Napolitano, I. Benedictis, A. M. Malfitano, M. Monti, M. Ravera, E. Gabano and D. Marasco, A Comparative Study of the Effects of Platinum(II) Complexes on beta-Amyloid Aggregation: Potential Neurodrug Applications, *Int. J. Mol. Sci.*, 2021, **22**, 3015.

22 S. La Manna, V. Roviello, V. Monaco, J. A. Platts, M. Monti, E. Gabano, M. Ravera and D. Marasco, The inhibitory effects of platinum(II) complexes on amyloid aggregation: a theoretical and experimental approach, *Dalton Trans.*, 2023, **52**, 12677–12685.

23 S. La Manna, M. Leone, I. Iacobucci, A. Annuziata, C. Di Natale, E. Lagreca, A. M. Malfitano, F. Ruffo, A. Merlino and M. Monti, Glucosyl platinum(II) complexes inhibit aggregation of the C-terminal region of the Aβ peptide, *Inorg. Chem.*, 2022, **61**, 3540–3552.

24 Z. Xu, Z. Wang, Z. Deng and G. Zhu, Recent advances in the synthesis, stability, and activation of platinum(IV) anticancer prodrugs, *Coord. Chem. Rev.*, 2021, **442**, 213991.

25 M. Shahlaei, S. M. Asl, A. Derakhshani, L. Kurek, J. Karges, R. Macgregor, M. Saeidifar, I. Kostova and A. A. Saboury, Platinum-based drugs in cancer treatment: Expanding horizons and overcoming resistance, *J. Mol. Struct.*, 2023, 137366.

26 D. Gibson, Multi-action Pt(IV) anticancer agents; do we understand how they work?, *J. Inorg. Biochem.*, 2019, **191**, 77–84.

27 V. B. Kenche, L. W. Hung, K. Perez, I. Volitakes, G. Ciccotosto, J. Kwok, N. Critch, N. Sherratt, M. Cortes and V. Lal, Development of a platinum complex as an anti-amyloid agent for the therapy of Alzheimer's disease, *Angew. Chem.*, 2013, **125**, 3458–3462.

28 M. Ravera, E. Gabano, M. J. McGlinchey and D. Osella, Pt (IV) antitumor prodrugs: dogmas, paradigms, and realities, *Dalton Trans.*, 2022, **51**, 2121–2134.

29 E. Gabano, M. B. Gariboldi, G. Caron, G. Ermondi, E. Marras, M. Vallaro and M. Ravera, Application of the anthraquinone drug rhein as an axial ligand in bifunctional Pt(IV) complexes to obtain antiproliferative agents against human glioblastoma cells, *Dalton Trans.*, 2022, **51**, 6014–6026.

30 C. Wu, H. Cao, H. Zhou, L. Sun, J. Xue, J. Li, Y. Bian, R. Sun, S. Dong, P. Liu and M. Sun, Research Progress on the Antitumor Effects of Rhein: Literature Review, *Adv. Anticancer Agents Med. Chem.*, 2017, **17**, 1624–1632.

31 R. Pei, Y. Jiang, G. Lei, J. Chen, M. Liu and S. Liu, Rhein derivatives, a promising pivot?, *Mini-Rev. Med. Chem.*, 2021, **21**, 554–575.

32 P. P. Pagare, S. A. Zaidi, X. Zhang, X. Li, X. Yu, X. Y. Wang and Y. Zhang, Understanding molecular interactions between scavenger receptor A and its natural product inhibitors through molecular modeling studies, *J. Mol. Graphics Modell.*, 2017, **77**, 189–199.

33 Y. Yuan, X. Li, S. A. Zaidi, C. K. Arnatt, X. Yu, C. Guo, X.-Y. Wang and Y. Zhang, Small molecule inhibits activity of scavenger receptor A: lead identification and preliminary studies, *Bioorg. Med. Chem. Lett.*, 2015, **25**, 3179–3183.

34 K. Murakami, T. Yoshioka, S. Horii, M. Hanaki, S. Midorikawa, S. Taniwaki, H. Gunji, K.-i. Akagi, T. Kawase and K. Hirose, Role of the carboxy groups of triterpenoids in their inhibition of the nucleation of amyloid β42 required for forming toxic oligomers, *Chem. Commun.*, 2018, **54**, 6272–6275.

35 C. Di Natale, S. La Manna, A. M. Malfitano, S. Di Somma, D. Florio, P. L. Scognamiglio, E. Novellino, P. A. Netti and D. Marasco, Structural insights into amyloid structures of the C-terminal region of nucleophosmin 1 in type A mutation of acute myeloid leukemia, *Biochim. Biophys. Acta, Proteins Proteomics*, 2019, **1867**, 637–644.

36 S. La Manna, P. L. Scognamiglio, V. Roviello, F. Borbone, D. Florio, C. Di Natale, A. Bigi, C. Cecchi, R. Cascella, C. Giannini, T. Sibillano, E. Novellino and D. Marasco, The acute myeloid leukemia-associated Nucleophosmin 1 gene mutations dictate amyloidogenicity of the C-terminal domain, *FEBS J.*, 2019, **286**, 2311–2328.

37 S. La Manna, D. Florio, C. Di Natale, F. Napolitano, A. M. Malfitano, P. A. Netti, I. De Benedictis and D. Marasco, Conformational consequences of NPM1 rare mutations: An aggregation perspective in Acute Myeloid Leukemia, *Bioorg. Chem.*, 2021, **113**, 104997.

38 S. La Manna, C. Di Natale, V. Panzetta, M. Leone, F. A. Mercurio, I. Cipollone, M. Monti, P. A. Netti, G. Ferraro and A. Terán, A diruthenium metallodrug as a potent inhibitor of amyloid-β aggregation: synergism of mechanisms of action, *Inorg. Chem.*, 2023, **63**, 564–575.

39 S. La Manna, V. Panzetta, C. Di Natale, I. Cipollone, M. Monti, P. A. Netti, A. Terán, A. E. Sánchez-Peláez, S. Herrero and A. Merlino, Comparative Analysis of the

Inhibitory Mechanism of Aβ1–42 Aggregation by Diruthenium Complexes, *Inorg. Chem.*, 2024, **63**, 10001–10010.

40 P. Krupa, P. D. Quoc Huy and M. S. Li, Properties of monomeric Aβ42 probed by different sampling methods and force fields: Role of energy components, *J. Chem. Phys.*, 2019, **151**, 055101.

41 H. L. Nguyen, P. Krupa, N. M. Hai, H. Q. Linh and M. S. Li, Structure and physicochemical properties of the Aβ42 tetramer: multiscale molecular dynamics simulations, *J. Phys. Chem. B*, 2019, **123**, 7253–7269.

42 C. Di Natale, S. La Manna, C. Avitabile, D. Florio, G. Morelli, P. A. Netti and D. Marasco, Engineered beta-hairpin scaffolds from human prion protein regions: Structural and functional investigations of aggregates, *Bioorg. Chem.*, 2020, **96**, 103594.

43 S. Dhara, A rapid method for the synthesis of cis-[Pt (NH3) 2Cl2], *Indian J. Chem.*, 1970, **8**, 193–194.

44 M. Ravera, E. Gabano, I. Zanellato, F. Fregonese, G. Pelosi, J. A. Platts and D. Osella, Antiproliferative activity of a series of cisplatin-based Pt(IV)-acetylamido/carboxylato prodrugs, *Dalton Trans.*, 2016, **45**, 5300–5309.

45 E. Gabano, I. Zanellato, G. Pinton, L. Moro, M. Ravera and D. Osella, The Strange Case: The Unsymmetric Cisplatin–Based Pt(IV) Prodrug [Pt (CH_3COO) Cl2 (NH3) 2 (OH)] Exhibits Higher Cytotoxic Activity with respect to Its Symmetric Congeners due to Carrier–Mediated Cellular Uptake, *Bioinorg. Chem. Appl.*, 2022, **2022**, 3698391.

46 O. Korb, T. Stutzle and T. E. Exner, Empirical scoring functions for advanced protein– ligand docking with PLANTS, *J. Chem. Inf. Model.*, 2009, **49**, 84–96.

47 G. R. Navale, I. Ahmed, M. H. Lim and K. Ghosh, Transition Metal Complexes as Therapeutics: A New Frontier in Combatting Neurodegenerative Disorders through Protein Aggregation Modulation, *Adv. Healthcare Mater.*, 2024, **13**, 2401991.